New Journal of Physics
The open-access journal for physics

The Talbot effect for a surface plasmon polariton

A A Maradudin and T A Leskova

Department of Physics and Astronomy and Institute for Surface and Interface Science, University of California, Irvine, CA 92697, USA
E-mail: aamaradu@uci.edu and tleskova@uci.edu

New Journal of Physics **11** (2009) 033004 (9pp)
Received 31 December 2008
Published 3 March 2009
Online at http://www.njp.org/
doi:10.1088/1367-2630/11/3/033004

Abstract. On the basis of an impedance boundary condition, we study theoretically the transmission of a surface plasmon polariton incident normally on a periodic row of circular metallic or dielectric dots deposited on a planar metallic substrate. The field of the transmitted surface plasmon polaritons displays periodic self-images of this row that are separated from it by multiples of a characteristic distance. This is the analogue for surface plasmon polaritons of the Talbot effect for volume electromagnetic waves.

When light is transmitted through a one-dimensional periodic structure, the image of that structure is found to repeat itself periodically with increasing distance of the image plane from the structure. This self-imaging of the periodic structure was discovered by H F Talbot in 1836 [1], and has been the subject of many subsequent theoretical and experimental investigations[1].

As in the case of other effects originally associated with volume electromagnetic waves whose analogues have begun to be studied in the context of surface electromagnetic waves, such as negative refraction [3] and cloaking [4], the analogue of the Talbot effect has recently been studied theoretically for surface plasmon polaritons [2]. The system studied by Dennis *et al* consisted of a periodic row of holes drilled in a metal film and illuminated from the back side. Periodic images of this row in the intensity distribution of the total transmitted field on the front side of the film were produced, which were separated from the original one by multiples of a characteristic length.

In this paper, we study theoretically the Talbot effect for surface plasmon polaritons on the basis of a rather different system from the one considered by Dennis *et al*, and by a rather different approach. The system we study should be as simple as theirs to fabricate. It consists

[1] A good list of references to studies of the Talbot effect is contained in the paper by Dennis *et al* [2].

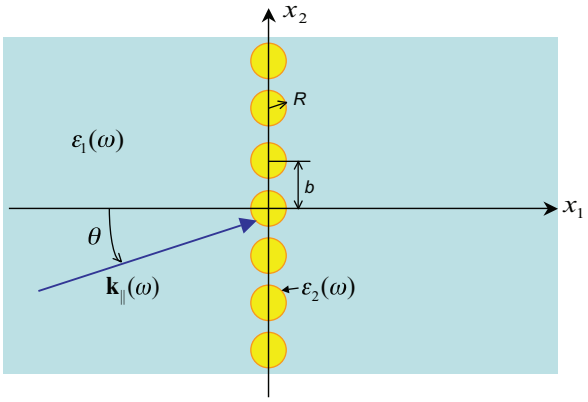

Figure 1. The geometry under study.

of vacuum in the region $x_3 > 0$ and a metal characterized by a dielectric function $\epsilon_1(\omega)$ in the region $x_3 < 0$. Deposited on this surface is a periodic row of dots of a material characterized by a dielectric function $\epsilon_2(\omega)$ (figure 1). The radius of each dot is R, and they are centered at the points $(0, nb, 0)$, where $n = 0, \pm 1, \pm 2, \ldots$. We assume that $R < b/2$, so that the dots do not overlap. The interface between vacuum and the metal whose dielectric function is $\epsilon_1(\omega)$ supports a surface plasmon polariton of frequency ω. A surface plasmon polariton of this frequency is incident on this row of dots from the region $x_1 < 0$. The scattering and transmission of the incident surface plasmon polariton by this structure are studied on the basis of an impedance boundary condition [5] on the surface $x_3 = 0$, which can be successfully used for metals [5] and for strongly reflecting dielectric surfaces [6]. We write this boundary condition in the form $(i, j = 1, 2)$

$$\mathbf{J}_E(\mathbf{x}_\parallel|\omega)_i = K_{ij}^{(0)}(\mathbf{x}_\parallel|\omega)\mathbf{J}_H(\mathbf{x}_\parallel|\omega)_j, \tag{1}$$

where summation over repeated subscripts is assumed. In equation (1), we have introduced the vectors $\mathbf{J}_E(\mathbf{x}_\parallel|\omega) = \hat{\mathbf{x}}_3 \times \mathbf{E}^>(\mathbf{x}|\omega)|_{x_3=0}$ and $\mathbf{J}_H(\mathbf{x}_\parallel|\omega) = \hat{\mathbf{x}}_3 \times \mathbf{H}^>(\mathbf{x}|\omega)|_{x_3=0}$, where $\mathbf{E}^>(\mathbf{x}|\omega)$ $(\mathbf{H}^>(\mathbf{x}|\omega))$ is the total electric (magnetic) field in the vacuum region $x_3 > 0$, and the caret over a vector denotes a unit vector. The only nonzero elements of the surface impedance tensor $\overleftrightarrow{K}^{(0)}(\mathbf{x}_\parallel\omega)$ are

$$\begin{aligned} K_{12}^{(0)}(\mathbf{x}_\parallel|\omega) &= \kappa_1(\omega) + (\kappa_2(\omega) - \kappa_1(\omega))S(\mathbf{x}_\parallel) \\ &= -K_{21}^{(0)}(\mathbf{x}_\parallel|\omega), \end{aligned} \tag{2}$$

where

$$S(\mathbf{x}_\parallel) = \sum_{n=-\infty}^{\infty} \theta(R - |\mathbf{x}_\parallel - \hat{\mathbf{x}}_2 nb|), \tag{3}$$

$\theta(x)$ is the Heaviside unit step function and $\kappa_j(\omega) = \mathrm{i}/(-\epsilon_j(\omega))^{1/2}$.

The incident surface plasmon polariton is p polarized. The total electric and magnetic fields $\mathbf{E}^{>}(\mathbf{x}|\omega)$ and $\mathbf{H}^{>}(\mathbf{x}|\omega)$, respectively, are then given by

$$\mathbf{E}^{>}(\mathbf{x}|\omega) = \frac{c}{\omega}[\mathrm{i}\hat{\mathbf{k}}_{\parallel}(\omega)\beta_0(\omega) - \hat{\mathbf{x}}_3 k_{\parallel}(\omega)]\exp[\mathrm{i}\mathbf{k}_{\parallel}(\omega)\cdot\mathbf{x}_{\parallel} - \beta_0(\omega)x_3]$$
$$+ \int \frac{\mathrm{d}^2 q_{\parallel}}{(2\pi)^2}\exp[\mathrm{i}\mathbf{q}_{\parallel}\cdot\mathbf{x}_{\parallel} - \beta_0(q_{\parallel})x_3]$$
$$\times\left\{\frac{c}{\omega}[\mathrm{i}\hat{\mathbf{q}}_{\parallel}\beta_0(q_{\parallel}) - \hat{\mathbf{x}}_3 q_{\parallel}]A_{\parallel}(\mathbf{q}_{\parallel}) + (\hat{\mathbf{x}}_3\times\hat{\mathbf{q}}_{\parallel})A_{\perp}(\mathbf{q}_{\parallel})\right\}, \tag{4a}$$

$$\mathbf{H}^{>}(\mathbf{x}|\omega) = (\hat{\mathbf{x}}_3\times\hat{\mathbf{k}}_{\parallel}(\omega))\exp[\mathrm{i}\mathbf{k}_{\parallel}(\omega)\cdot\mathbf{x}_{\parallel} - \beta_0(\omega)x_3]$$
$$+\int\frac{\mathrm{d}^2 q_{\parallel}}{(2\pi)^2}\exp[\mathrm{i}\mathbf{q}_{\parallel}\cdot\mathbf{x}_{\parallel} - \beta_0(q_{\parallel})x_3]\left\{(\hat{\mathbf{x}}_3\times\hat{\mathbf{q}}_{\parallel})A_{\parallel}(\mathbf{q}_{\parallel}) - \frac{c}{\omega}[\mathrm{i}\hat{\mathbf{q}}_{\parallel}\beta_0(q_{\parallel}) - \hat{\mathbf{x}}_3 q_{\parallel}]A_{\perp}(\mathbf{q}_{\parallel})\right\}. \tag{4b}$$

A time dependence $\exp(-\mathrm{i}\omega t)$ has been assumed for these fields, but has not been indicated explicitly.

The first term on the right-hand side of equations (4*a*) and (4*b*) gives the field of the incident surface plasmon polariton. It has the form of an evanescent plane wave whose angle of incidence measured counterclockwise from the negative x_1-axis is θ. The vector $\mathbf{k}_{\parallel}(\omega)$ is given by $\mathbf{k}_{\parallel}(\omega) = k_{\parallel}(\omega)(\cos\theta, \sin\theta, 0)$, where $k_{\parallel}(\omega) = (\omega/c)[1 - 1/\epsilon_1(\omega)]^{1/2}$ is the solution of the dispersion relation, in the impedance approximation, for surface plasmon polaritons at the planar interface between vacuum and a metal whose dielectric function is $\epsilon_1(\omega)$, namely

$$[k_{\parallel}^2(\omega) - (\omega/c)^2]^{1/2} + \mathrm{i}(\omega/c)\kappa_1(\omega) = 0. \tag{5}$$

The function $\beta_0(\omega)$ is given by $\beta_0(\omega) = (\omega/c)(-\epsilon_1(\omega))^{-1/2}$.

The integral term on the right-hand side of equations (4*a*) and (4*b*) gives the scattered field, consisting of the surface plasmon polariton reflected/transmitted by the periodic row of dots, and volume waves radiated into the vacuum. Here $\beta_0(q_{\parallel}) = [q_{\parallel}^2 - (\omega/c)^2]^{1/2}$ with $\mathrm{Re}\,\beta_0(q_{\parallel}) > 0$, $\mathrm{Im}\,\beta_0(q_{\parallel}) < 0$ and the coefficients $A_{\parallel}(\mathbf{q}_{\parallel})$ and $A_{\perp}(\mathbf{q}_{\parallel})$ are the amplitudes of the p- and s-polarized components of the scattered field with respect to the local sagittal plane defined by the vectors $\hat{\mathbf{q}}_{\parallel}$ and $\hat{\mathbf{x}}_3$. They are functions of the vector $\mathbf{k}_{\parallel}(\omega)$, but we do not indicate this explicitly.

When we substitute equations (4) into equation (1) and make use of equation (2), we obtain a pair of coupled integral equations for $A_{\parallel}(\mathbf{q}_{\parallel})$ and $A_{\perp}(\mathbf{q}_{\parallel})$, which can be written in the form

$$\left[\mathrm{i}(c/\omega)\beta_0(p_{\parallel}) - \kappa_1(\omega)\right]A_{\parallel}(\mathbf{p}_{\parallel}) - (\kappa_2(\omega) - \kappa_1(\omega))\int\frac{\mathrm{d}^2 q_{\parallel}}{(2\pi)^2}\hat{S}(\mathbf{p}_{\parallel} - \mathbf{q}_{\parallel})$$
$$\times\left\{(\hat{\mathbf{p}}_{\parallel}\cdot\hat{\mathbf{q}}_{\parallel})A_{\parallel}(\mathbf{q}_{\parallel}) - \mathrm{i}(\hat{\mathbf{p}}_{\parallel}\times\hat{\mathbf{q}}_{\parallel})_3\frac{c}{\omega}\beta_0(q_{\parallel})A_{\perp}(\mathbf{q}_{\parallel})\right\}$$
$$= (\kappa_2(\omega) - \kappa_1(\omega))(\hat{\mathbf{p}}_{\parallel}\cdot\hat{\mathbf{k}}_{\parallel})\hat{S}(\mathbf{p}_{\parallel} - \mathbf{k}_{\parallel}), \tag{6a}$$

$$\left[-1+\mathrm{i}(c/\omega)\kappa_1(\omega)\beta_0(p_\parallel)\right]A_\perp(\mathbf{p}_\parallel)+(\kappa_2(\omega)-\kappa_1(\omega))\int\frac{\mathrm{d}^2q_\parallel}{(2\pi)^2}\hat{S}(\mathbf{p}_\parallel-\mathbf{q}_\parallel)$$
$$\times\left\{(\hat{\mathbf{p}}_\parallel\times\hat{\mathbf{q}}_\parallel)_3A_\parallel(\mathbf{q}_\parallel)+\mathrm{i}(\hat{\mathbf{p}}_\parallel\cdot\hat{\mathbf{q}}_\parallel)\frac{c}{\omega}\beta_0(q_\parallel)A_\perp(\mathbf{q}_\parallel)\right\}$$
$$=-(\kappa_2(\omega)-\kappa_1(\omega))(\hat{\mathbf{p}}_\parallel\times\hat{\mathbf{k}}_\parallel)_3\hat{S}(\mathbf{p}_\parallel-\mathbf{k}_\parallel). \tag{6b}$$

The vector $\mathbf{p}_\parallel=(p_1,\,p_2,\,0)$ in these equations is an arbitrary vector in the plane $x_3=0$. The function $\hat{S}(\mathbf{Q}_\parallel)$ is defined by

$$\hat{S}(\mathbf{Q}_\parallel)=\int\mathrm{d}^2x_\parallel S(\mathbf{x}_\parallel)\exp(-\mathrm{i}\mathbf{Q}_\parallel\cdot\mathbf{x}_\parallel), \tag{7}$$

and we have omitted the argument ω of the vector $\mathbf{k}_\parallel(\omega)$. Since in the present case $S(\mathbf{x}_\parallel)$ is defined by equation (3), we find that

$$\hat{S}(\mathbf{Q}_\parallel)=\sum_{m=-\infty}^{\infty}2\pi\delta(Q_2-(2\pi m/b))s_m(Q_1) \tag{8a}$$

with

$$s_m(Q_1)=\frac{2\pi R^2}{b}\frac{J_1(\sqrt{(Q_1^2+(2\pi m/b)^2}R)}{\sqrt{Q_1^2+(2\pi m/b)^2}R}, \tag{8b}$$

where $J_1(x)$ is a Bessel function of the first kind and first order.

The vanishing of the coefficient of $A_\parallel(\mathbf{p}_\parallel)$ on the left-hand side of equation (6*a*) is the dispersion relation for surface plasmon polaritons at the planar interface between vacuum and a metal whose dielectric function is $\epsilon_1(\omega)$ (equation (5)). This means that the coefficient $A_\parallel(\mathbf{p}_\parallel)$ has a resonant nature. It is preferable to work with integral equations for smoothly varying functions rather than for resonant functions, so we introduce new amplitudes $\tilde{A}_\parallel(\mathbf{p}_\parallel)$ and $\tilde{A}_\perp(\mathbf{p}_\parallel)$ by

$$A_\parallel(\mathbf{p}_\parallel)=\frac{\tilde{A}_\parallel(\mathbf{p}_\parallel)}{\beta_0(p_\parallel)+\mathrm{i}(\omega/c)\kappa_1(\omega)}, \tag{9a}$$

$$A_\perp(\mathbf{p}_\parallel)=\frac{\tilde{A}_\perp(\mathbf{p}_\parallel)}{(\omega/c)-\mathrm{i}\kappa_1(\omega)\beta_0(p_\parallel)}. \tag{9b}$$

Each of these new amplitudes is a smoothly varying function of $\mathbf{p}_\parallel$. The equations they satisfy are

$$\tilde{A}_\parallel(\mathbf{p}_\parallel)-b(\omega)\int\frac{\mathrm{d}^2q_\parallel}{(2\pi)^2}\hat{S}(\mathbf{p}_\parallel-\mathbf{q}_\parallel)\left\{\frac{(\hat{\mathbf{p}}_\parallel\cdot\hat{\mathbf{q}}_\parallel)}{\beta_0(q_\parallel)-a(\omega)}\tilde{A}_\parallel(\mathbf{q}_\parallel)-\frac{\mathrm{i}(\hat{\mathbf{p}}_\parallel\times\hat{\mathbf{q}}_\parallel)_3\beta_0(q_\parallel)}{(\omega/c)^2+a(\omega)\beta_0(q_\parallel)}\tilde{A}_\perp(\mathbf{q}_\parallel)\right\}$$
$$=b(\omega)(\hat{\mathbf{p}}_\parallel\cdot\hat{\mathbf{k}}_\parallel)\hat{S}(\mathbf{p}_\parallel-\mathbf{k}_\parallel), \tag{10a}$$

$$\tilde{A}_\perp(\mathbf{p}_\parallel)-b(\omega)\int\frac{\mathrm{d}^2q_\parallel}{(2\pi)^2}\hat{S}(\mathbf{p}_\parallel-\mathbf{q}_\parallel)\left\{\frac{\mathrm{i}(\hat{\mathbf{p}}_\parallel\times\hat{\mathbf{q}}_\parallel)_3}{\beta_0(q_\parallel)-a(\omega)}\tilde{A}_\parallel(\mathbf{q}_\parallel)-\frac{(\hat{\mathbf{p}}_\parallel\cdot\hat{\mathbf{q}}_\parallel)\beta_0(q_\parallel)}{(\omega/c)^2+a(\omega)\beta_0(q_\parallel)}\tilde{A}_\perp(\mathbf{q}_\parallel)\right\}$$
$$=\mathrm{i}b(\omega)(\hat{\mathbf{p}}_\parallel\times\hat{\mathbf{k}}_\parallel)_3\hat{S}(\mathbf{p}_\parallel-\mathbf{k}_\parallel), \tag{10b}$$

where, to simplify the notation, we have defined $a(\omega) \equiv -\mathrm{i}(\omega/c)\kappa_1(\omega)$ and $b(\omega) \equiv -\mathrm{i}(\omega/c)(\kappa_2(\omega) - \kappa_1(\omega))$.

Moreover, because of the periodicity of our system in the x_2-direction, we introduce the expansion

$$\tilde{A}_{\parallel,\perp}(\mathbf{q}_\parallel) = \sum_{n=-\infty}^{\infty} 2\pi\delta(q_2 - k_2 - (2\pi n/b))a_{\parallel,\perp}^{(n)}(q_1) \tag{11}$$

to ensure the satisfaction of the Floquet–Bloch theorem. On substituting equation (11) into equation (10), we obtain the equations satisfied by the amplitudes $\{a_{\parallel,\perp}^{(n)}(q_1)\}$:

$$\begin{aligned} a_\parallel^{(m)}(p_1) - b(\omega) &\int_{-\infty}^{\infty} \frac{\mathrm{d}q_1}{2\pi} \sum_{n=-\infty}^{\infty} s_{m-n}(p_1 - q_1) \\ &\times \left[\frac{\hat{\mathbf{p}}_m \cdot \hat{\mathbf{q}}_n}{\beta_n(q_1) - a(\omega)} a_\parallel^{(n)}(q_1) - \mathrm{i}\frac{(\hat{\mathbf{p}}_m \times \hat{\mathbf{q}}_n)_3 \beta_n(q_1)}{(\omega/c)^2 + a(\omega)\beta_n(q_1)} a_\perp^{(n)}(q_1) \right] \\ &= b(\omega)\hat{\mathbf{p}}_m \cdot \hat{\mathbf{k}}_\parallel s_m(p_1 - k_1), \qquad m = 0, \pm 1, \pm 2, \ldots, \end{aligned} \tag{12a}$$

$$\begin{aligned} a_\perp^{(m)}(p_1) - b(\omega) &\int_{-\infty}^{\infty} \frac{\mathrm{d}q_1}{2\pi} \sum_{n=-\infty}^{\infty} s_{m-n}(p_1 - q_1) \\ &\times \left[\frac{\mathrm{i}(\hat{\mathbf{p}}_m \times \hat{\mathbf{q}}_n)_3}{\beta_n(q_1) - a(\omega)} a_\parallel^{(n)}(q_1) + \frac{(\hat{\mathbf{p}}_m \cdot \hat{\mathbf{q}}_n)\beta_n(q_1)}{(\omega/c)^2 + a(\omega)\beta(q_1)} a_\perp^{(n)}(q_1) \right] \\ &= \mathrm{i}b(\omega)(\hat{\mathbf{p}}_m \times \hat{\mathbf{k}}_\parallel)_3 s_m(p_1 - k_1), \qquad m = 0, \pm 1, \pm 2, \ldots. \end{aligned} \tag{12b}$$

In writing these equations, we have introduced the definitions $k_{2m} = k_2 + (2\pi m/b)$, $\mathbf{p}_m = (p_1, k_{2m}, 0)$, $p_m = (p_1^2 + k_{2m}^2)^{1/2}$, $\beta_0((p_1^2 + k_{2m}^2)^{1/2}) = \beta_0(p_m) = \beta_m(p_1)$ and $\mathbf{q}_n = (q_1, k_{2n}, 0)$, $q_n = (q_1^2 + k_{2n}^2)^{1/2}$, $\beta_0((q_1^2 + k_{2n}^2)^{1/2}) = \beta_0(q_n) = \beta_n(q_1)$.

Equations (12) are solved numerically by converting them into a pair of coupled matrix equations by replacing the infinite range of integration by a finite range $(-Q, Q)$, and evaluating the resulting integrals by the extended midpoint method [7].

The electric vector of the scattered field is given by the second term on the right-hand side of equation (4*a*). The contribution to this field from surface plasmon polaritons is given by the residues of the poles of the integrand corresponding to the zeros of $\beta_n(q_1) - a(\omega)$. Thus in the region $x_1 > 0$, the electric field associated with surface plasmon polaritons becomes

$$\begin{aligned} \mathbf{E}^>(\mathbf{x}|\omega)_{\mathrm{spp}} = &\frac{c}{\omega}[\mathrm{i}\hat{\mathbf{k}}_\parallel \beta_0(\omega) - \hat{\mathbf{x}}_3 k_\parallel] \exp(\mathrm{i}\mathbf{k}_\parallel \cdot \mathbf{x}_\parallel - \beta_0(\omega)x_3) + \mathrm{i}a(\omega)\exp[-\beta_0(\omega)x_3] \\ &\times \sum_n \frac{c}{\omega}\left(\mathrm{i}\hat{\mathbf{k}}_n \beta_0(\omega) - \hat{\mathbf{x}}_3 k_\parallel\right) \frac{a_\parallel^{(n)}((k_\parallel^2 - k_{2n}^2)^{1/2})}{(k_\parallel^2 - k_{2n}^2)^{1/2}} \exp\left[\mathrm{i}(k_\parallel^2 - k_{2n}^2)^{1/2}x_1 + \mathrm{i}k_{2n}x_2\right], \end{aligned} \tag{13}$$

where the sum runs over only those values of n for which $|k_{2n}| < k_\parallel$. The coefficients of x_1 and x_2 in the exponential function in the summand define a vector whose magnitude is $k_\parallel$ for each value of n.

Up to now we have considered the general case where the angle of incidence of the incoming surface plasmon polariton has the nonzero value θ. We now specialize the preceding results to the case of normal incidence, for which $\theta = 0$, so that $k_2 = 0$. It follows that $k_{2n} = (2\pi n/b)$ in this case. Equation (13) then takes the form

$$\begin{aligned}\mathbf{E}^{>}(\mathbf{x}|\omega)_{\mathrm{spp}} = {} & \frac{c}{\omega}\exp(\mathrm{i}k_{\parallel}x_1 - \beta_0(\omega)x_3)\left(\mathrm{i}\beta_0(\omega), 0, -k_{\parallel}\right) \\ & + \mathrm{i}a(\omega)\exp(-\beta_0(\omega)x_3)\sum_n \frac{a_{\parallel}^{(n)}((k_{\parallel}^2 - (2\pi n/b)^2)^{1/2})}{(k_{\parallel}^2 - (2\pi n/b)^2)^{1/2}} \\ & \times \exp\left[\mathrm{i}\left(k_{\parallel}^2 - (2\pi n/b)^2\right)^{1/2}x_1 + \mathrm{i}(2\pi n/b)x_2\right] \\ & \times \frac{c}{\omega}\left(\mathrm{i}\frac{\beta_0(\omega)}{k_{\parallel}}\left(k_{\parallel}^2 - (2\pi n/b)^2\right)^{1/2}, \mathrm{i}\frac{\beta_0(\omega)}{k_{\parallel}}(2\pi n/b), -k_{\parallel}\right). \end{aligned} \tag{14}$$

If in the exponent in the summand in this expression we make the paraxial approximation ($k_{\parallel} \gg (2\pi n/b)$), we can use the expansion $(k_{\parallel}^2 - (2\pi n/b)^2)^{1/2} = k_{\parallel} - (2\pi^2 n^2/k_{\parallel}b^2) + \cdots$ to simplify equation (14) to

$$\begin{aligned}\mathbf{E}^{>}(\mathbf{x}|\omega)_{\mathrm{spp}} = {} & \frac{c}{\omega}\exp(\mathrm{i}k_{\parallel}x_1 - \beta_0(\omega)x_3)\left(\mathrm{i}\beta_0(\omega), 0, -k_{\parallel}\right) \\ & + \mathrm{i}a(\omega)\exp[\mathrm{i}k_{\parallel}x_1 - \beta_0(\omega)x_3]\sum_n \frac{a_{\parallel}^{(n)}((k_{\parallel}^2 - (2\pi n/b)^2)^{1/2})}{(k_{\parallel}^2 - (2\pi n/b)^2)^{1/2}} \\ & \times \exp\left[-\mathrm{i}\left(2\pi n^2/\tau\right)x_1 + \mathrm{i}(2\pi n/b)x_2\right] \\ & \times \frac{c}{\omega}\left(\mathrm{i}\frac{\beta_0(\omega)}{k_{\parallel}}\left(k_{\parallel}^2 - (2\pi n/b)^2\right)^{1/2}, \mathrm{i}\frac{\beta_0(\omega)}{k_{\parallel}}(2\pi n/b), -k_{\parallel}\right), \end{aligned} \tag{15}$$

where $\tau = k_{\parallel}b^2/\pi$ is the Talbot distance. If we denote the vector defined by the sum in equation (15) by $\mathbf{F}(x_1, x_2|\omega)$, we see that it possesses the properties

$$\mathbf{F}(0, x_2|\omega) = \mathbf{F}(\tau, x_2|\omega), \tag{16a}$$

$$\mathbf{F}(\tau/2, x_2|\omega) = \mathbf{F}(0, x_2 - b/2|\omega). \tag{16b}$$

We note that the self-imaging effect described by equations (16) is strictly a consequence of the paraxial approximation $k_{\parallel} \gg (2\pi n/b)$. Nevertheless, as we will see, the effect survives to a good approximation even when the condition for the paraxial approximation is slightly relaxed.

To illustrate these results, we consider the case where the frequency of the incident surface plasmon polariton corresponds to a vacuum wavelength $\lambda = 1.55\,\mu$m. The dielectric function $\epsilon_1(\omega)$ at this wavelength is $\epsilon_1(\omega) = -130.83 + \mathrm{i}3.32$ (silver), so that the surface plasmon wavelength $\lambda_{\mathrm{sp}} = 2\pi/\mathrm{Re}(k_{\parallel}(\omega))$ is $\lambda_{\mathrm{sp}} = 1.544\,\mu$m, and its energy propagation length $\ell_{\mathrm{sp}} = 1/(2\,\mathrm{Im}(k_{\parallel}(\omega)))$ is $\ell_{\mathrm{sp}} \approx 1.28$ mm. We consider here two types of the dot material, namely, gold dots (the dielectric function $\epsilon_2(\omega) = -95.92 + \mathrm{i}10.76$) and silicon dots (the dielectric function $\epsilon_2(\omega) = 12$). In figure 2, we present a color-level plot of $|E_3^{>}(\mathbf{x}|\omega)_{\mathrm{spp}}|$ as a function of x_1 and x_2 when $x_3 = 0$ for the case where the surface plasmon polariton is scattered by a row of dielectric dots with periods $b = \lambda_{\mathrm{sp}}$ (a), $b = 10\lambda_{\mathrm{sp}}$ (b) and $b = 20\lambda_{\mathrm{sp}}$ (c). In each case, the radius of the dot is $R = b/3$. The Talbot distance is $\tau = 12.5\,\mu$m (a), $\tau = 1.26$ mm (b) and $\tau = 5$ mm (c). In figure 3, we present a color-level plot of $|E_3^{>}(\mathbf{x}|\omega)_{\mathrm{spp}}|$ as a function of x_1 and

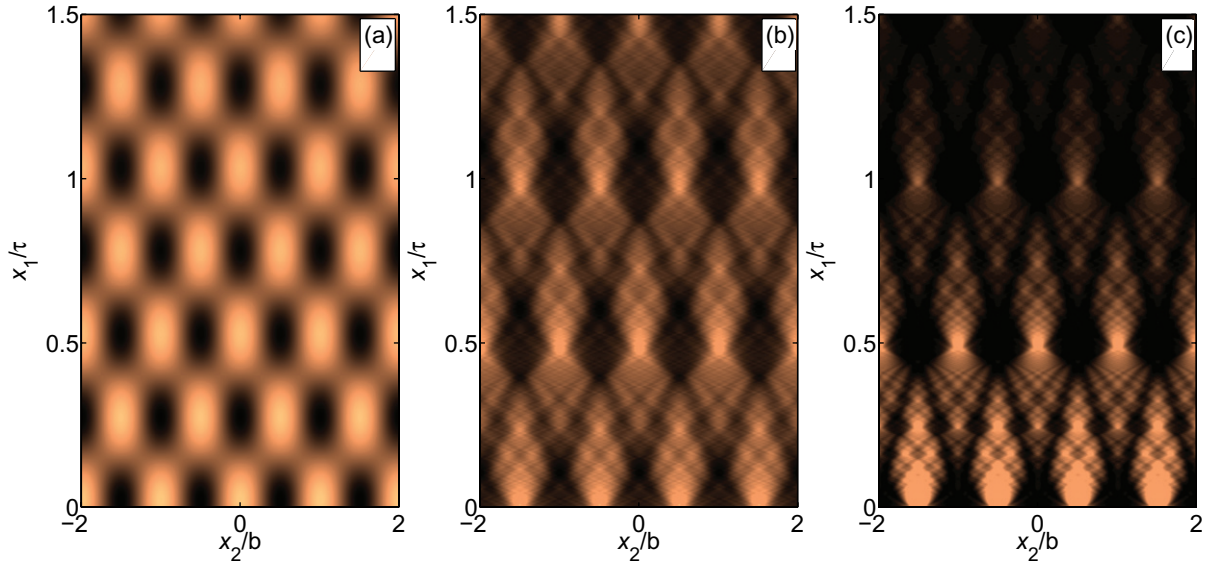

Figure 2. A color-level plot of $|E_3^{>}(\mathbf{x}|\omega)_{\mathrm{spp}}|$ as a function of x_1 and x_2 when $x_3 = 0$ when a surface plasmon polariton propagates along a silver surface and is scattered by a row of silicon dots of a period $b = \lambda_{\mathrm{sp}}$ (a), $b = 10\lambda_{\mathrm{sp}}$ (b) and $b = 20\lambda_{\mathrm{sp}}$ (c). The radius of each dot is $R = b/3$.

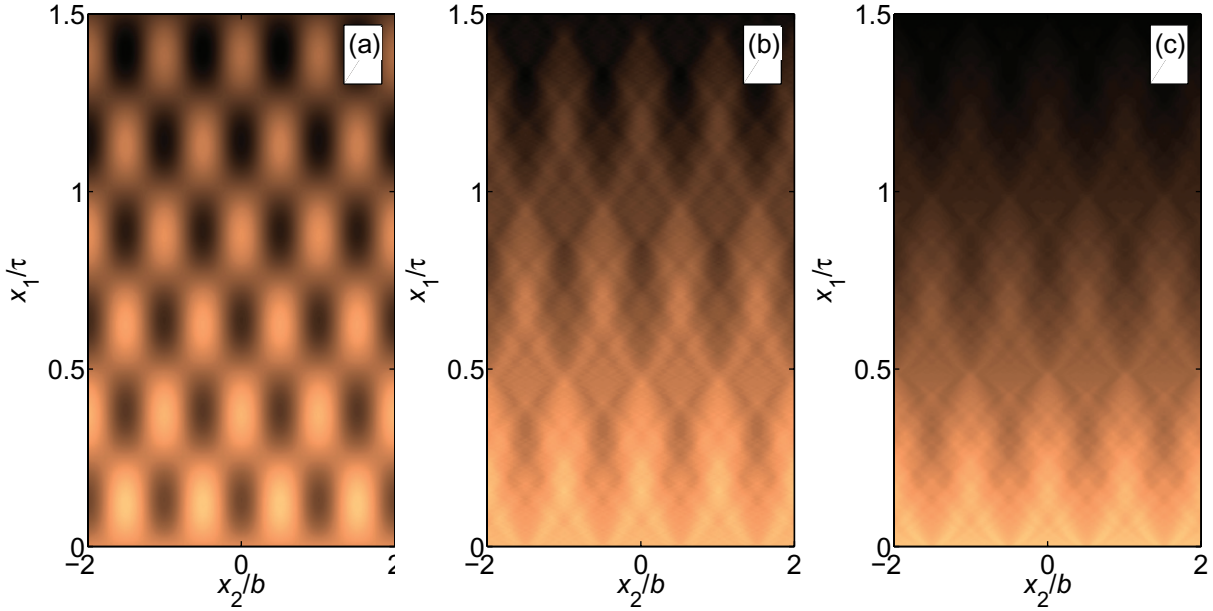

Figure 3. The same as in figure 2, but for the case where a surface plasmon polariton propagates along a silver surface and is scattered by a row of gold dots.

x_2 when $x_3 = 0$ calculated for the same parameters as were used in obtaining figure 2, but for the case where a surface plasmon polariton propagates along a silver surface and is scattered by a row of gold dots.

The self-imaging effect described by equations (16) is clearly seen in both scattering geometries, even for a period as small as $b = 10\lambda_{\mathrm{sp}}$, as well as the formation of the Talbot

carpet that results from sub-images formed at regular fractions of the Talbot length smaller than $\frac{1}{2}$. The stronger the scattering the more pronounced is the complicated structure of the diffraction pattern. In the scattering geometry considered here, the smaller the scatterers the stronger the zero (specular)-order beam of the surface plasmon polaritons and, as a result, the smaller the contrast of the Talbot carpet. The stronger scattering is also the reason for the much more complicated pattern in the case of scattering by a row of dielectric dots than in the case of a row of metallic dots. Since the propagation length of surface plasmon polaritons is about the Talbot distance in the case where the period of the structure is $b = 10\lambda_{sp}$, in the case where the period $b = 20\lambda_{sp}$ the Talbot carpet is practically washed out on the scale of the Talbot distance (figures 2(c) and 3(c)). We note here that in contrast to the results of Dennis *et al* [2] only the contribution from the field of surface plasmon polaritons is taken into account in calculations of the interference pattern. In the geometry considered in our paper, the conversion of the incident surface plasmon polariton into the volume waves is weak. The color-level plots presented in figures 2(a) and 3(a) show a period that is half of the Talbot distance. In this case, the period of the surface structure is $b = \lambda_{sp}$, so that there are only the (0) and ($\pm$1) order beams of the transmitted surface plasmon polariton, and the ($\pm$1) order beams propagate along the x_2-axis. Therefore, in this case, the period of the interference pattern is determined by the wavelength λ_{sp} rather than by the Talbot distance, which is $\tau = 2\lambda_{sp}$ in this case.

Thus, on the basis of an impedance boundary condition approach, we have studied theoretically the transmission of a surface plasmon polariton incident normally on a periodic row of dots formed from either a metal that is different from the substrate or from a dielectric. The transmitted surface plasmon polariton field displays periodic self-images of this row that are separated from the original row by multiples of the characteristic Talbot distance, $\tau = k_{\|}b^2/\pi$. The approach used in obtaining this result can be useful in studies of the interaction of surface plasmon polaritons with other surface structures.

Just as the Talbot effect for volume electromagnetic waves has been used in a variety of applications (see for example [8]–[12]), it can be expected that its analogue for surface plasmon polaritons will find applications in a variety of nanoscale plasmonic devices.

A structured surface of the kind studied here can be fabricated in the following manner. A metal film ($\epsilon_1(\omega)$) whose thickness is greater than the penetration depth of a surface plasmon polariton into that metal is evaporated onto a glass substrate. A periodic row of holes of finite depth and radius R is then drilled in the film at the points $(0, nb, 0)$ with $n = 0, \pm1, \pm2, \ldots$ by, e.g. a photon scanning tunneling microscope/direct-write lithography setup [13]. These holes are then filled by a second medium ($\epsilon_2(\omega)$) by vacuum deposition through a mask.

The incident surface plasmon polariton can be excited by a prism coupler [14], by a grating coupler [15], or by illumination of the gap between the edge of a razor blade and the metal surface [16], for example. An optical image of the near-field distribution of the intensity of the transmitted surface plasmon polaritons can be obtained, e.g. by means of a photon scanning tunneling microscope [13].

Acknowledgments

We thank Dr Dan-Hong Huang for asking the question that led to this paper. This research was supported in part by AFRL contract AF 9453-08-C-0230.

References

[1] Talbot H F 1836 Facts relating to optical science, no. IV *Phil. Mag.* **9** 401–7

[2] Dennis M R, Zheludev N I and García de Abajo F J 2007 The plasmon Talbot effect *Opt. Express* **15** 9692–700

[3] Shin H and Fan S 2006 All-angle negative refraction for surface plasmon waves using a metal–dielectric–metal structure *Phys. Rev. Lett.* **96** 073907

[4] Smolyaninov I I, Hung Y J and Davis C C 2008 Two-dimensional metamaterial structure exhibiting reduced visibility at 500 nm *Opt. Lett.* **33** 1342–4

[5] Maradudin A A 1995 The impedance boundary condition at a two-dimensional rough metal surface *Opt. Commun.* **116** 452–67

[6] Maradudin A A and Méndez E R 1996 The utility of an impedance boundary condition in the scattering of light from one-dimensional randomly rough dielectric surfaces *Opt. Spectrosc.* **80** 409–20

[7] Press W H, Teukolsky S A, Vetterling W T and Flannery B P 1992 *Numerical Recipes in Fortran* 2nd edn (New York: Cambridge University Press) p 129

[8] Patorski K 1989 The self-imaging phenomenon and its applications *Prog. Opt.* **27** 3–101

[9] Lohmann A W and Thomas J A 1990 Making an array illuminator based on the Talbot effect *Appl. Opt.* **29** 4337–40

[10] Smolyaninov I I and Davis C C 1998 Apparent superresolution in near-field optical imaging of periodic gratings *Opt. Lett.* **23** 1346–7

[11] Moon E E, Chen L, Everett P N, Mondol M K and Smith H I 2004 Nanometer gap measurement and verification via chirped-Talbot effect *J. Vac. Sci. Technol.* B **22** 3378–81

[12] Garcia-Sucerquia J, Alvarez-Palacio D C and Kreuzer H J 2008 High resolution Talbot self-imaging applied to structural characterization of self-assembled monolayers of microspheres *Appl. Opt.* **47** 4723–8

[13] Smolyaninov I I, Mazzoni D L and Davis C C 1996 Imaging of surface plasmon scattering by lithographically created individual surface defects *Phys. Rev. Lett.* **77** 3877–80

[14] Otto A 1968 Excitation of nonradiative surface plasma waves in silver by the method of frustrated total reflection *Z. Phys.* **216** 398–410

[15] Beaglehole D 1969 Coherent and incoherent radiation from optically excited surface plasmons on a metal grating *Phys. Rev. Lett.* **22** 708–11

[16] Zhizhin G N, Moskaleva M A, Shomina E V and Yakovlev V A 1979 Edge effects due to propagation of surface IR electromagnetic waves along a metal surface *JETP Lett.* **29** 486–9